Human Molecular Genetics, 2007, Vol. 16, No. 15 **1802–1813**
doi:10.1093/hmg/ddm128
Advance access published on May 21, 2007

Rai1 deficiency in mice causes learning impairment and motor dysfunction, whereas *Rai1* heterozygous mice display minimal behavioral phenotypes

Weimin Bi[1], Jiong Yan[1], Xin Shi[1], Lisa A. Yuva-Paylor[1], Barbara A. Antalffy[2], Alica Goldman[3], Jong W. Yoo[3], Jeffrey L. Noebels[1,3], Dawna L. Armstrong[2], Richard Paylor[1,5] and James R. Lupski[4,6,*]

[1]Department of Molecular and Human Genetics, [2]Department of Pathology, [3]Department of Neurology, [4]Department of Pediatrics, [5]Department of Neuroscience, Baylor College of Medicine, Houston, TX, USA and [6]Texas Children's Hospital, Houston, TX, USA

Received April 2, 2007; Revised and Accepted May 4, 2007

Smith–Magenis syndrome (SMS) is associated with an ~3.7 Mb common deletion in 17p11.2 and characterized by its craniofacial and neurobehavioral abnormalities. The reciprocal duplication leads to dup(17)(p11.2p11.2) associated with the Potocki–Lupski syndrome (PLS), a neurological disorder whose features include autism. *Retinoic acid induced 1* (*RAI1*) appears to be responsible for the majority of clinical features in both SMS and PLS. Mouse models of these syndromes harboring an ~2 Mb chromosome engineered deletion and duplication, respectively, displayed abnormal locomotor activity and/or learning deficits. To determine the contribution of *RAI1* in the neurobehavioral traits in SMS, we performed a battery of behavioral tests on *Rai1* mutant mice and the *Df(11)17 − 1/+* mice that have a small deletion of ~590 kb. The mice with the small deletion were hypoactive like the large deletion mice and they also showed learning deficits. The *Rai1 +/−* mice exhibited normal locomotor activity. However, they had an abnormal electroencephalogram with overt seizure observed in a subset of mice. The few surviving *Rai1 −/−* mice displayed more severe neurobehavioral abnormalities including hind limb clasping, overt seizures, motor impairment and context- and tone-dependant learning deficits. X-gal staining of the *Rai1 +/−* mice suggests that *Rai1* is predominantly expressed in neurons of the hippocampus and the cerebellum. Our results suggest that *Rai1* is a critical gene in the central nervous system functioning in a dosage sensitive manner and that the neurobehavioral phenotype is modified by regulator(s) in the ~590 kb genomic interval, wherein the major modifier affecting the craniofacial penetrance resides.

INTRODUCTION

Smith–Magenis syndrome (SMS, MIM 18829) is a multiple congenital abnormalities/mental retardation disorder with characteristic craniofacial and neurobehavioral manifestations (1–4). The minimum prevalence of SMS is 1 in 25 000 births (5). Individuals with SMS usually have low adaptive functioning with relative strengths in socialization and relative weakness in daily living skills (6), mild-to-moderate mental retardation (1) and display a characteristic neurobehavioral pattern of stereotypes, self-injurious and maladaptive behaviors (4). More than 70% of SMS cases harbor an ~3.7 Mb common deletion mediated by non-allelic homologous recombination using flanking low copy repeats as substrates (7).

A critical region for SMS (SMCR) was confined to an ~1.1 Mb genomic interval by breakpoint junction analysis in SMS patients with unusual smaller-sized deletions (8). Twenty genes were found in the SMCR, 19 of which are also found in the syntenic 32–34 cM region of mouse

*To whom correspondence should be addressed at: Department of Molecular and Human Genetics, Baylor College of Medicine, Room 604B, One Baylor Plaza, Houston, TX 77030-3498, USA. Tel: +1 7137986530; Fax: +1 7137985073; Email: jlupski@bcm.tmc.edu

Table 1. Comparison of phenotypes in mouse models of Smith–Magenis and Potocki–Lupski syndromes

Features		*Df(11)17/+* Δ(*Csn3–Zfp179*)	*Df(11)17 − 1/+* Δ(*Csn3–4933439F18Rik*)	*Rai1 +/−*	*Rai1 −/−*	*Dp(11)17/+* dup(*Csn3–Zfp179*)
Craniofacial abnormalities		+, 70–80%	+, 48%	+, 18%	+, 100%	−
Obesity		+	+	+	−	−
Reduced male fertility		+	−	−	+	−
T4 deficiency		+	NA	NA	NA	NA
Neurobehavioral abnormalities						
Overt seizures		+, 20%	NA	+, 2%	+, 30%	−
Abnormal EEG		+	NA	+	+	−
Abnormal circadian rhythm		+	NA	NA	NA	−
Imparied fear conditioning	Context dependant	−	+	−	+	+
	Tone dependant	−	+	−	+	−
Locomotor activity	Hypoactive	+	+	−	−	−
	Hyperactive	−	−	−	−	+

The *Df(11)17/+* (22,25), *Df(11)17 − 1/+* (24), *Rai1 +/−* (21) and *Dp(11)17/+* (14,22,25) mice were characterized in the N2 generation (75% C57BL/6 / 25% 129SvEv), whereas the *Rai1 −/−* mice were studied in the F2 generation (50% C57BL/6 / 50% 129SvEv). 'NA' means not assessed yet.

chromosome 11 (8). The order and orientation of each of these 19 genes are conserved between humans and mice (8,9). Mutations in a gene within the SMCR, *retinoic acid induced 1* (*RAI1*), were identified in nine patients with typical SMS features but no FISH detectable deletions (10–13). These patients displayed characteristic SMS craniofacial and neurobehavioral phenotypes indicating that *RAI1* is the major causative gene. Studies on mouse models (14) suggest that *RAI1* is likely the dosage sensitive gene responsible for clinical features in the Potocki–Lupski (PLS) MIM610883 dup(17)(p11.2p11.2) syndrome, a neurobehavioral disorder with autistic features that is caused by reciprocal duplication of the same region commonly deleted in the SMS (15–17).

RAI1 contains a polymorphic CAG repeat that encodes a polyglutamine stretch in its N-terminus. RAI1 has been implicated in neurobehavioral traits as evidenced by the findings that the length of the CAG repeats has been associated with two neurological diseases; modification of the age at onset for spinocerebellar ataxia type 2 (SCA2) (18) and response to neuroleptic drugs in patients with schizophrenia (19). A single plant homeo domain (PHD) zinc finger, frequently observed in chromatin remodeling transcriptional regulators, is present in the C-terminus of both human and mouse *RAI1* (10). Murine *Rai1* has only two glutamines instead of a polyglutamine stretch, but it shares 86% similarity with its human homologue. The expression of *Rai1*, previously named *GT1*, was stimulated by the treatment of retinoic acid in embryonic carcinoma cells and it is expressed in neurons specifically in the brain (20). During embryogenesis, *Rai1* is predominantly expressed in the epithelial cells involved in organogenesis (21).

To further understand the etiology of SMS through animal studies, we have constructed several mouse models of SMS and PLS: the *Df(11)17/+* mice (Del mutant) harboring a large ∼2 Mb deleted region syntenic to the common SMS deletion, whereas the *Dp(11)17/+* mice (Dup mutant) contain a reciprocal duplication created by chromosome engineering (22), the *Df(11)17–4/+* mice having a deletion of ∼1 Mb (23), the *Df(11)17 − 1/+* mice having a small deletion of ∼590 kb (24), and *Rai1* deficient mice containing an insertionally inactivated allele generated by gene targeting (21). About 25 genes were deleted in the large deletion mice, whereas only 11 genes were deleted in the mice with the small or ∼590 kb deletion. We have characterized and compared the craniofacial features and growth of these mouse models at the N2 generation. Table 1 summarizes the phenotypes in different mouse models.

Del mutant mice partially recapitulate the SMS features, exhibiting craniofacial abnormalities, seizures and obesity. In addition, the Del mutants displayed hypoactivity and abnormal circadian rhythm, while the Dup mutants that have a reciprocal duplication were hyperactive and have impaired contextual fear conditioning. Similar craniofacial defects and obesity were also observed in three lines of mice harboring a smaller deletion (∼590 kb) (24) and the mice with inactivation of the *Rai1* gene by gene targeting (21). Importantly, in a congenic C57BL/6 background, Del mice and the smaller deletion mice had a similar penetrance, whereas that of *Rai1 +/−* mice was significantly lower, which suggested the existence of a major genetic modifier(s) in the 590 kb interval surrounding *Rai1* affecting the craniofacial penetrance (23). It is unknown how the dosage insufficiency of *Rai1* affects the mammalian behaviors and what the contribution of *Rai1* is in the behavioral phenotypes observed in the Del mouse models.

To explore the role of *RAI1* in SMS and its function in the nervous system, we performed a battery of behavioral tests on both the mice with a small ∼ 590 kb deletion and *Rai1 +/−* mice and compared their behaviors with those observed in the mice with a large 2 Mb deletion in the same genetic background. We also evaluated the behaviors of the *Rai1 −/−* mice and the expression profile of *Rai1* in the nervous system. In addition, we examined the clinically observed seizures in the *Rai1* mutant mice by electrophysiological methods using video-electroencephalograph (VEEG). Our data indicated that *Rai1* is strongly expressed in a subset of neurons in the brain and is required for motor function and learning ability. In addition, our results suggest that other major genetic modifier(s) for the behavioral phenotype in SMS resides in the 590 kb genomic interval deleted in the small deletion mice.

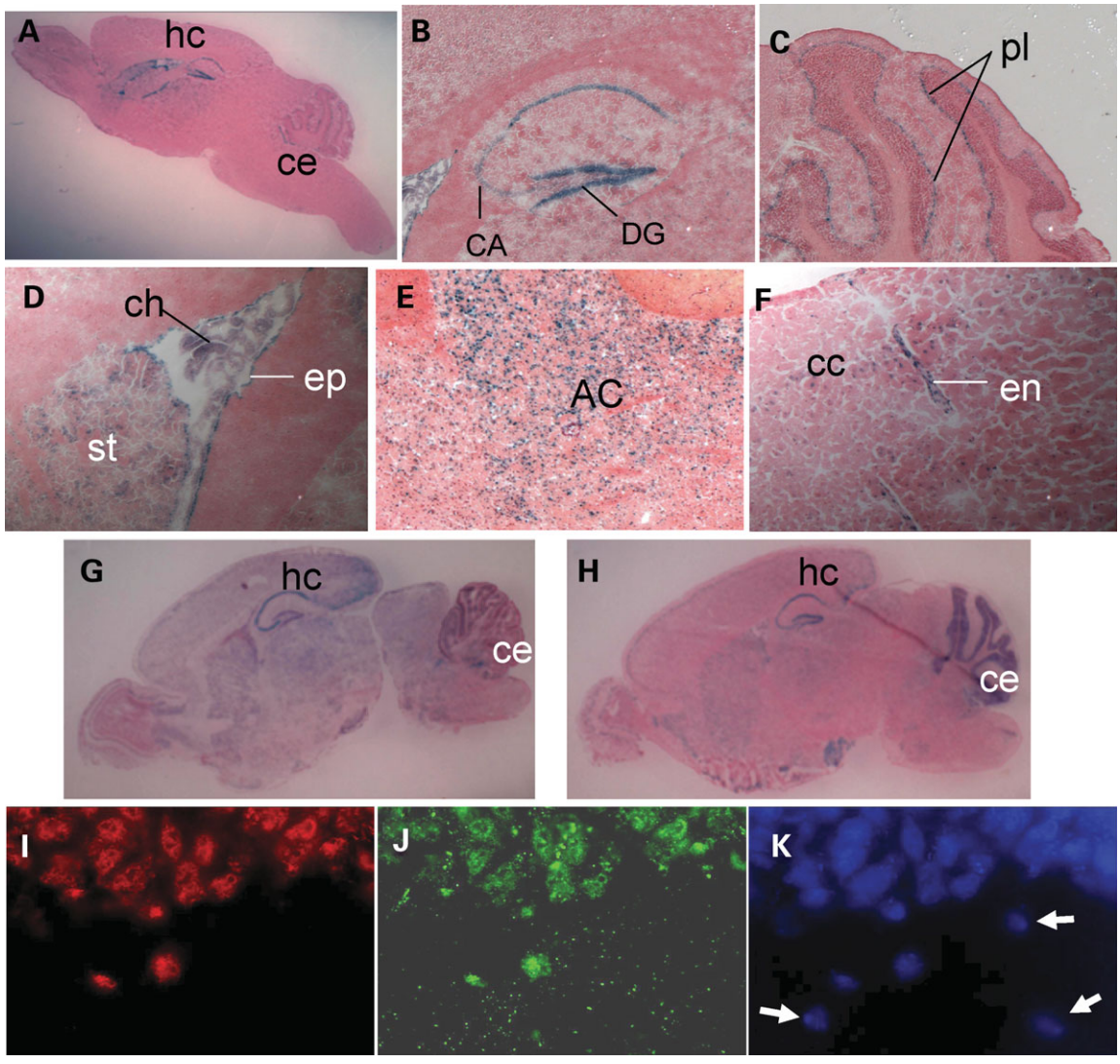

Figure 1. Expression of *Rai1* in mouse brain. (**A**–**H**) X-gal staining of sagittal brain sections prepared from *Rai1* +/− adult mice (A–F) and mice at d7 (G) and d20 (H). (A) A low magnification image to show that *Rai1* is predominantly expressed in the hippocampus (hc) and the cerebellum (ce). (B–F) High magnification to show the strong expression in the cornu ammonis (CA) and dentate gyrus (DG) of the hippocampus (B), Purkinje layer of the cerebellum (pl) (C), the ependyma (ep), the choroid plexus (ch) in the lateral ventricle, the striatum (st) (D), the nucleus accumbens (AC) (E), the cerebral cortex (cc) and endothelial cells (en) of blood vessels (F). (G–H) X-gal staining is generally broader during postnatal development than in adult mice. The strong expression in the hippocampus and cerebellum was observed in the brains of both d7 and d20 mice. (**I**–**K**) Neurons were indicated using anti-NeuN antibody (I) and expression of *Rai1* in neurons of the hippocampus was indicated by immunofluorescence using anti-lacZ antibodies (J). Nuclei were stained by DAPI (K). Note that the cells not stained by anti-NeuN antibody (indicated by arrows) were not stained by anti-lacZ antibody either.

RESULTS

Rai1 is strongly expressed in the central nervous system

We performed X-gal staining on frozen sections prepared from the brains of postnatal *Rai1* +/− mice that have a *lacZ* reporter gene knocked-into the *Rai1* gene. Blue-staining resulting from the inserted β-galactosidase, indicative of *Rai1* gene expression, was detected throughout the brain in low level and predominantly in the hippocampus and cerebellum (Fig. 1A), consistent with its *in situ* hybridization expression profile from the Allen Brain Atlas. In the hippocampus, the expression was observed in areas CA1, CA2, CA3 and the dentate gyrus (Fig. 1B). In the cerebellum, the expression was seen in the Purkinje layer (Fig. 1C). Other sites of strong expression include the striatum, neurons in the cerebral cortex, the nucleus accumbens, the epithelial membrane lining the ventricles of the brain, the ependyma and the choroid plexus (Fig. 1D–F). Expression of *Rai1* was also observed in the endothelial cells of blood vessels throughout the brain (Fig. 1F). In P7 and P20 stages, *Rai1* is expressed in a broader pattern in the developing brains and strong expression in the hippocampus and cerebellum was also observed (Fig. 1G and H). To examine which cells were stained in the central nervous system, we visualized neurons using anti-NeuN antibody and *Rai1* expression with anti-lacZ antibody. We found that the NeuN expressing cells also express *lacZ*,

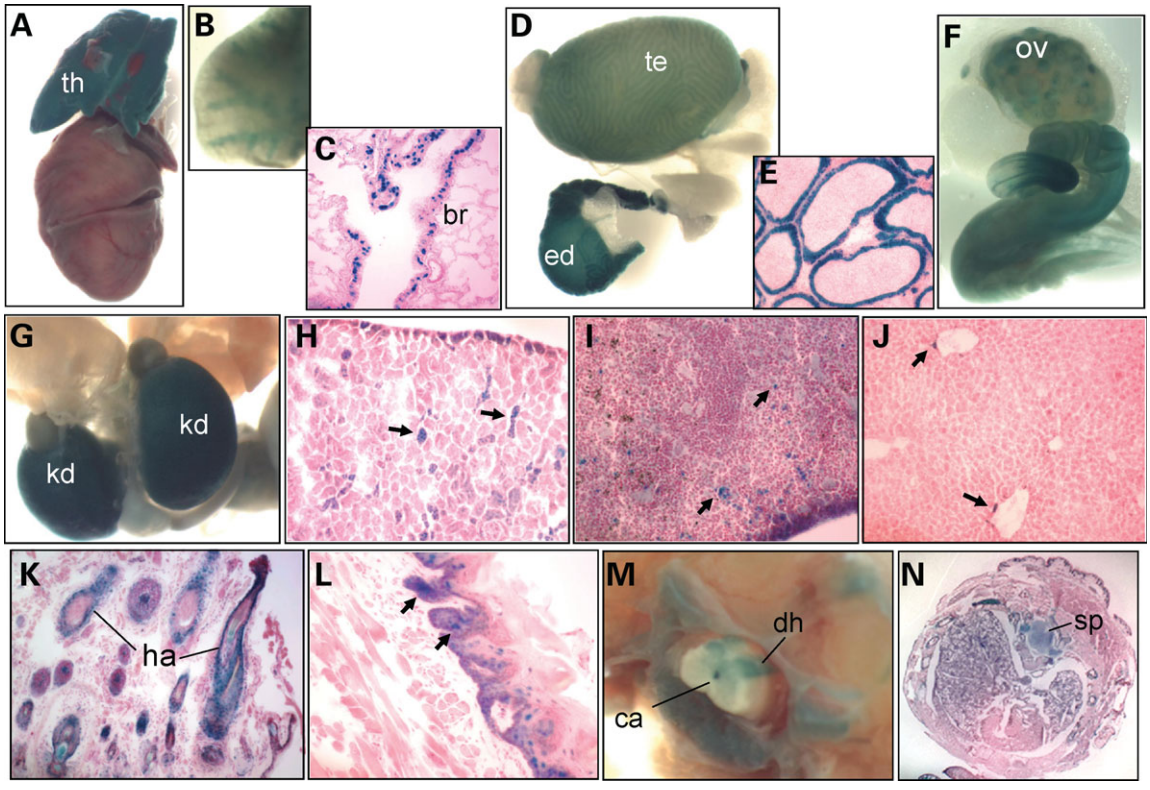

Figure 2. Expression of *Rai1* in organs visualized by X-gal staining of organs (**A**, **B**, **D**, **F**, **G**, **M**) and sections (**C**, **E**, **H**–**L**, **N**). Organs and tissues are from d1 mice for G, d20 mice for (A, D, E, K) and adult mice for (B and C, F, H–J, L, M). *Rai1* expression was observed in the thymus (th) (A), bronchiole (br) of the lung (B and C), the testis (te) (D), tubules of the epididymis (ed) (D and E), follicles in the ovary (ov) (F) and collecting tubules (arrows) of the kidney (kd) (G and H). Expression was also observed in a subset of cells (indicated by arrows) in the spleen (I) and liver (J), hair follicles (ha) in the skin (K), and the tongue (L). In the spinal cord, the central canal (ca) and the posterior horn (dh) of gray matter were blue stained (M). *Rai1* was well expressed in the developing spinal cord (sp) in E18.5 embryos (N).

suggesting that *Rai1* is expressed only in the neurons (Fig. 1I–K).

In addition to the brain, expression of *Rai1* was also observed in the thymus, bronchioles of the lung, collecting tubules in the kidney, the testis, the epididymis, the ovary, hair follicles in the skin, the tongue (Fig. 2). The mandibular gland and the intestine were well stained (data not shown). *Rai1* expression is low in the heart, the liver and the spleen with very few subsets of expressing cells. In adult mice, the central canal and the posterior horn of gray matter of the spinal cord were blue stained (Fig. 2M). The central canal is filled with the cerebrospinal fluid and *Rai1* is likely expressed in the ependymal cells similar to its expression in the ependyma in the brain. *Rai1* is well expressed in the developing spinal cord (Fig. 2N). In summary, *Rai1* is broadly expressed in multiple organs and tissues with variant expression levels in a subtype of tissues and cells.

Behavioral activities in mice with a small ∼590 kb deletion and *Rai1* +/− mice

The behavioral tests that showed significant differences between the *Df(11)17*/+ or *Dp(11)17*/+ mice and their wild-type littermates include the open-field test, light-dark test, prepulse inhibition of the acoustic startle response and the conditioned fear test (25). To understand the contribution of *Rai1* to the behavioral abnormalities, we performed the same behavioral tests on male mice with a small deletion, *Df(11)17 − 1*, and on the *Rai1* +/− male mice in a mixed background at the N2 (75% C57BL/6 and 25% 129SvEv) generation; a genetic background that is consistent with the Del mutants tested previously (25). We performed behavioral tests only on male mice because the behavioral phenotypes have better penetrance in male Del or Dup mice than in female mutant mice (22).

The open-field test was performed to measure locomotor activity and anxiety-related responses (26). In a novel arena, similar to the *Df(11)17* mice (25), the mice with the small deletion were hypoactive; they spent significantly less time moving ($P < 0.05$) and traveled a slightly shorter distance ($P = 0.17$) (Fig. 3A and B). They reared more than wild-type mice ($P = 0.05$) (Fig. 3C) and spent a higher proportion of their exploration in the center of the open field compared with the wild-type mice ($P < 0.05$) (Fig. 3D). In contrast, travel distance, travel time and center/total distance ratio of the *Rai1* +/− mutants were similar to that of the wild-type mice (Fig. 3A, B and D). The only significant difference between the *Rai1* +/− mutants and wild-type mice is that the vertical activity (rearing) was significantly increased in the *Rai1* +/− mice (Fig. 3C).

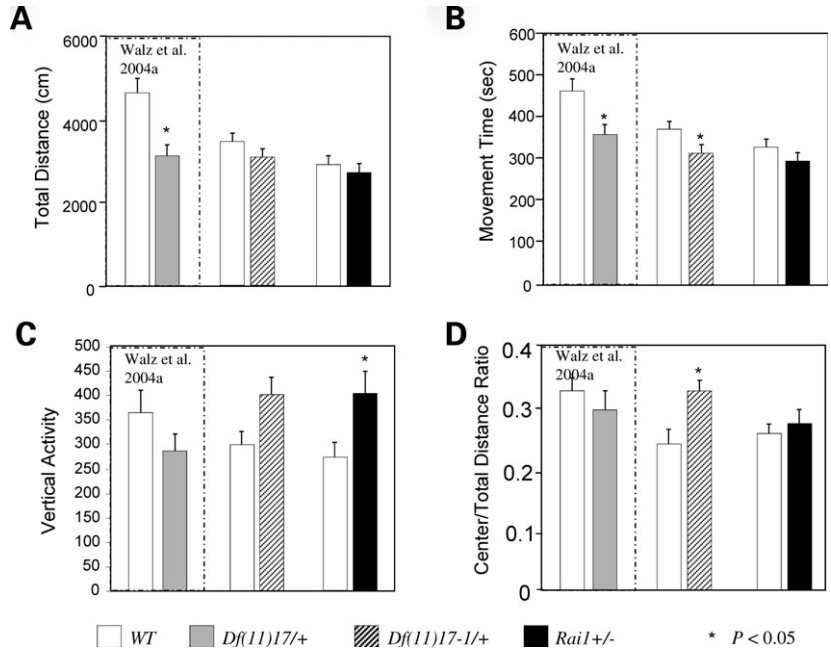

Figure 3. Open-field tests on *Df(11)17 − 1/+* mice with the smaller deletion and *Rai1 +/−* mice, as well as their wild-type littermates. The locomotor activities were measured by (**A**) total distance (cm), (**B**) movement time (s), (**C**) vertical activity, (**D**) center/total distance ratio. Mice with the small deletion spent less time traveling and spent more time in the center of the open-field arena. The *Rai1 +/−* mice reared significantly more than the wild-type. Values represent mean +/− SEM. Data of mice with the large deletion (25) are presented for comparison.

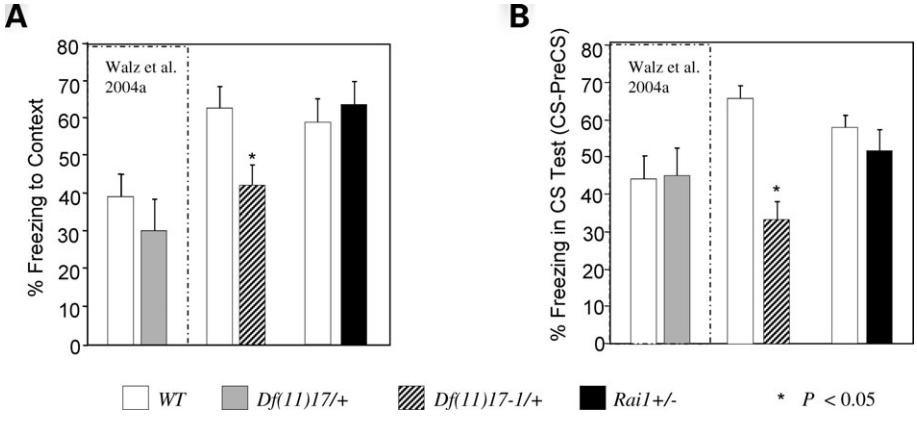

Figure 4. Conditioned fear test on *Df(11)17 − 1/+* mice with the small deletion and *Rai1 +/−* mice, as well as their wild-type littermates. The *Df(11)17 − 1/+* mice displayed freezing significantly less than wild-type mice in a context-dependant testing (**A**) and when presented with a tone in a novel context (**B**). The freezing behavior of *Rai1 +/−* mice is similar to that of wild-type mice. Values represent mean +/− SEM. Data of mice with the large deletion (25) are presented for comparison.

Individuals with SMS display different levels of cognitive deficits. We evaluated associative learning and memory in mice by the conditioned fear test, a fear-based response using a Pavlovian paradigm. The context-dependent fear conditioning is to test whether animals learned to associate a particular environment (context) with an aversive stimulus (an electric foot shock). In tone-dependent (cued) fear conditioning, the animals were tested to examine if they learned the association of an auditory stimulus with an aversive stimulus. The fear response to the presence of context or tone was a conditional freezing behavior characterized by a motionless, crouching posture and was assessed at 10 s intervals. The mice with a small deletion showed significantly less freezing without the conditioned stimulus (context test) ($P < 0.05$) and in the presence of conditioned stimulus (CS test) ($P < 0.05$) (Fig. 4). The *Rai1 +/−* mutants displayed levels of freezing behavior comparable with wild-type in both contextual and auditory cued conditioned fear tests (Fig. 4) consistent with the previous finding (14). Reduced freezing activity has been reported in the Dup mice in the context test but not in the CS test. However, the Del mice showed normal freezing in both context and CS tests (14,25).

Prepulse inhibition is a test to assess sensorimotor gating. For the maximum startle response, Dup mutant mice startled significantly less than wild-type mice (25). In contrast, the smaller deletion mice startled significantly more than

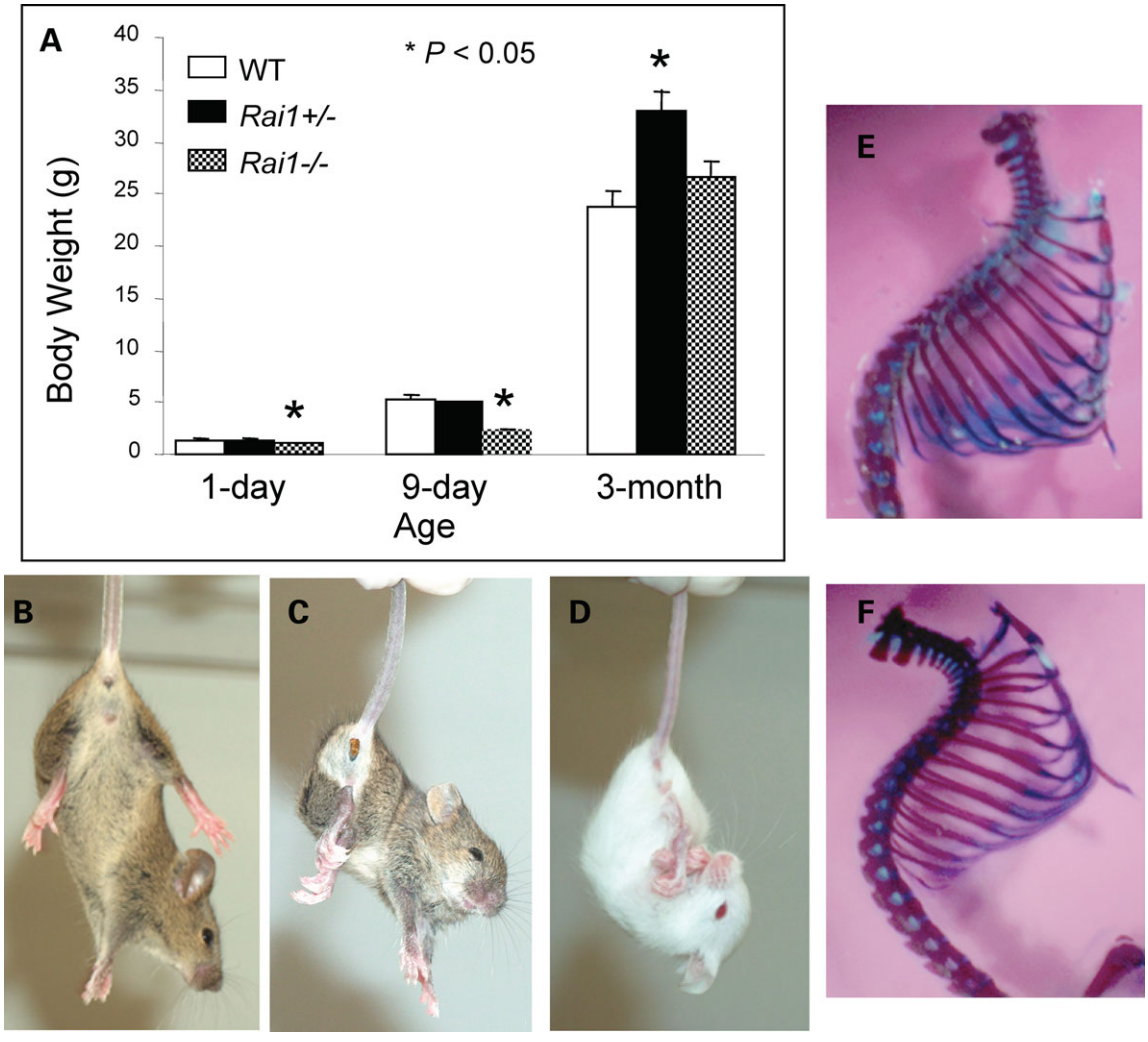

Figure 5. Phenotypes in the *Rai1* −/− mice that survived. (**A**) Growth chart to show that body weight of *Rai1* −/− female mice at 3 months of age was similar to their wild-type littermates although the mutants exhibited postnatal growth retardation (WT, $N = 4$; *Rai1* +/−, $N = 5$; *Rai1* −/−, $N = 6$). (**B**–**D**) Hind limb clasping observed in the *Rai1* −/− mice. When suspended by tail, the *Rai1* +/− mice clasped their hind limbs (C) or held their four limbs together (D), whereas the wild-type opened their hind legs widely (B). (**E** and **F**) Skeletal preparation to show that kyphosis was observed in some *Rai1* −/− mutants at ages over 4 months (F) while their wild-type littermates had a normal posture (E).

wild-type mice ($P < 0.05$), whereas there was no significant difference between *Rai1* +/− and wild-type mice (Supplementary Material, Fig. S1). There were no significant differences in the levels of prepulse inhibition for all genotypes (data not shown). Similar prepulse inhibition test results for *Rai1* +/− mice were reported previously (14).

The light–dark exploration test is used to assess anxiety-related responses. Similar to the Del mice with the large 2 Mb deletion, there were no significant differences in the mice with small deletion and the *Rai1* +/− mutants compared with wild-type mice in the light–dark test (Supplementary Material, Fig. S2).

Motor dysfunction and learning deficits in *Rai1* −/− mice

We previously reported that the vast majority of the *Rai1* −/− mice died during embryonic development (21). To explore the possibility of behavioral studies on *Rai1* −/− mice, we conducted large-scale breeding. We found that the body weight of the *Rai1* −/− mutants (female, $N = 4$) that survived is similar to wild-type mice at 3 months of age regardless of postnatal growth retardation (Fig. 5A). Approximately 10% of homozygous mutants at ages over 4 months displayed kyphosis (Fig. 5E and F). Microscopic studies on formalin fixed paraffin sections stained with hematoxylin and eosin revealed normal histology of the brain. The pyramidal cell layer in Ammon's horn and the granule cell layer in the dentate gyrus were well defined in the hippocampus of adult *Rai1* −/− mutants (data not shown).

When suspended by the tail, all the wild-type mice held their hind legs widely apart. We observed that all the *Rai1* −/− mutants consistently displayed hind limb clasping when suspended, which remained even after 3 months of age (Fig. 5B–D). They brought their hind limbs together (Fig. 5C) and some of them brought all four limbs together (Fig. 5D).

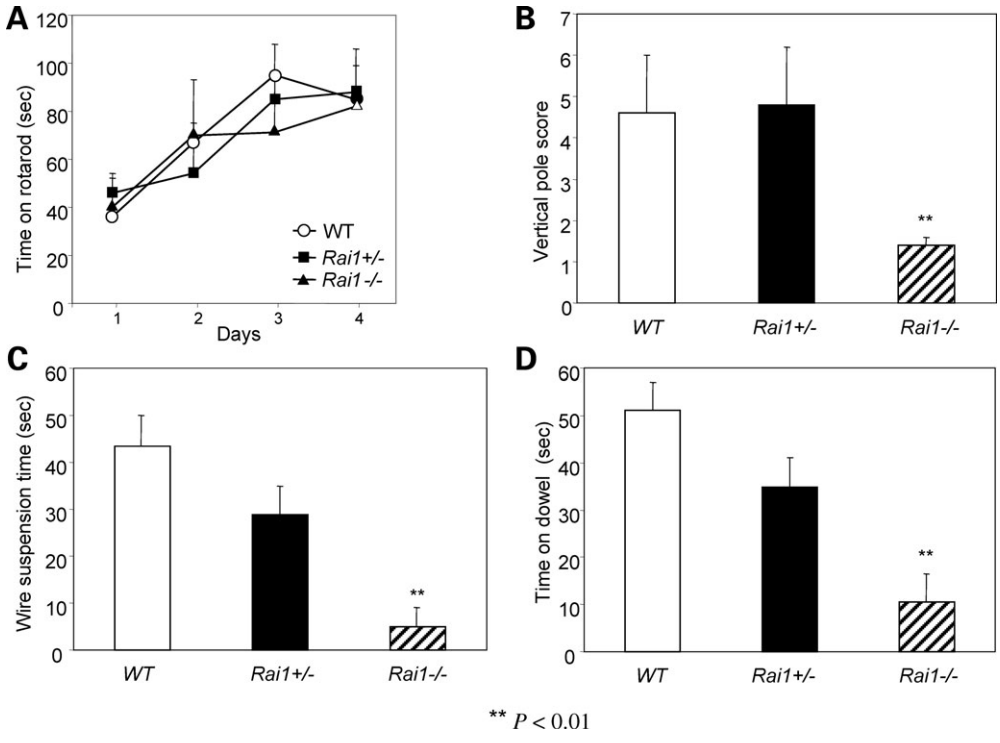

Figure 6. *Rai1* −/− mice displayed deficiency in motor skills. (**A**) The performance of the mutant mice is similar to the wild-type on an accelerating rotating rod. (**B**) The mutant mice were deficient in their ability to hold onto a pole that shifted from a horizontal to a vertical position. (**C** and **D**) The mutant mice hung onto a thin, metal wire by their forepaws (C) or remained in a wooden dowel (D) for a significantly shorter time than the wild-type. Values represent mean +/− SEM.

The hind limb clasping in the *Rai1* −/− mutants prompted us to evaluate their motor function using a battery of objective tests. Mice were evaluated on a rotating rod apparatus (rotarod) in which the speed of rotation was increased linearly from 4 to 40 rpm over 4 min. Both *Rai1* +/− and *Rai1* −/− mutants exhibited improvement in fall-off time during the 4-day period of testing and the mutants remained on the rotating rod for a time similar to wild-type mice (Fig. 6A). In the vertical pole test, mice were placed at the end of a horizontal pole and then the pole was lifted to a vertical position with mice at the top of the pole. *Rai1* −/− mice fell off the pole more readily and frequently than wild-type and heterozygous littermates significantly ($P = 0.009$) (Fig. 6B). We also analyzed the ability of mice to hold on to a wire with their forepaws in a wire suspension test. Whereas wild-type and heterozygous mice generally suspended in the wire for 30–60 s, *Rai1* −/− mice tended to fall off in <10 s ($P < 0.01$) (Fig. 6C). The ability of mice to remain on a thin, horizontal wooden dowel was tested. The wild-type and heterozygous mice were able to remain on the dowel for the maximum of 60 s. In contrast, the *Rai1* −/− mice lost their balance and fell off the dowel rapidly and usually in 11 s ($P < 0.001$) (Fig. 6D). These tests suggest that *Rai1* −/− mice have motor dysfunction.

Similar to the *Rai1* +/− mutants, there was no significant difference detected in the homozygous mutants for open-field test, light–dark test and prepulse inhibition with the exception that the *Rai1* −/− mutants showed significantly increased latency to enter as assessed in the light–dark test (data not shown). The levels of prepulse inhibition were similar between *Rai1* −/− mutants and wild-type mice, indicating that the sensorimotor gating appeared normal in the mutants. Interestingly, the *Rai1* homozygous mutants showed defective context-dependent as well as tone-dependent learning as evaluated by the conditioned fear tests (Fig. 7). Compared with the wild-type mice, the *Rai1* −/− mice demonstrated substantially less freezing behavior when placed in the test chamber without the conditioned stimulus (context test) ($P < 0.01$, in males only) and when in a modified chamber in the presence of the conditioned stimulus ($P < 0.05$, in both males and females) (Fig. 7). The decreased freezing behavior was also observed in the Dup mice and mice with the small deletion but not in Del mice and the *Rai1* +/− mice (Fig. 4) (25).

Seizures in the *Rai1* mutant mice

Overt seizures were observed in about one-third of *Rai1* −/− mutants after 3 months of age. Prolonged VEEG monitoring revealed an abnormal wake and sleep background punctuated by generalized spikes, multiple spikes and sharp waves. It was also noted that some of the events of sudden behavioral arrest correlated with electrographic seizures heralded by a generalized high voltage spike and slow wave complex followed by a 20-s long run of generalized 2.5–4 Hz spike and slow waves that evolved into a prolonged epoch of frontally dominant 6 Hz sharp waves (Fig. 8B). Overt generalized clonic–tonic–clonic seizures were observed as well. The electrographic patterns were characterized by an initial onset of

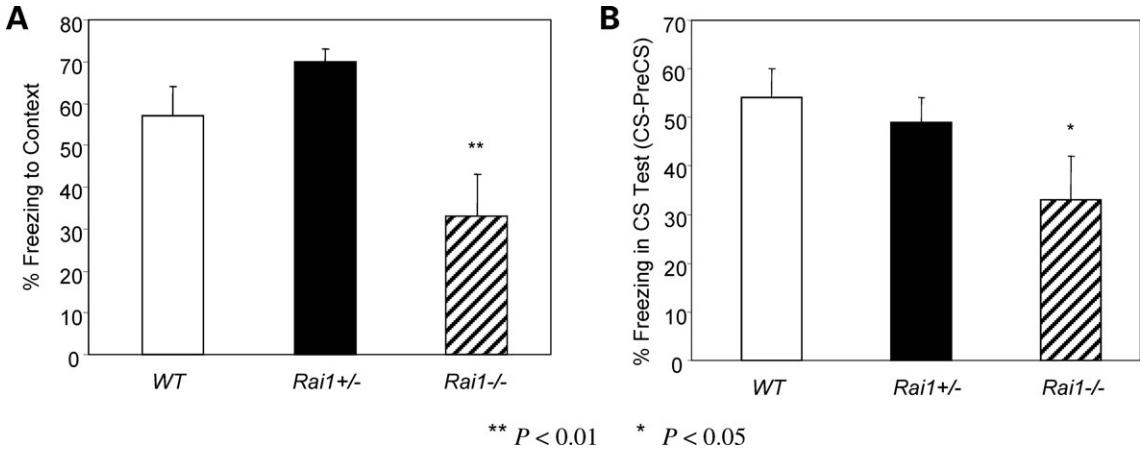

Figure 7. Learning deficiency in *Rai1* −/− mice evaluated by conditioned fear. *Rai1* −/− mice displayed freezing significantly less than the wild-type in a context-dependant test (**A**, for males only) and a tone-dependent test (**B**). Values represent mean +/− SEM.

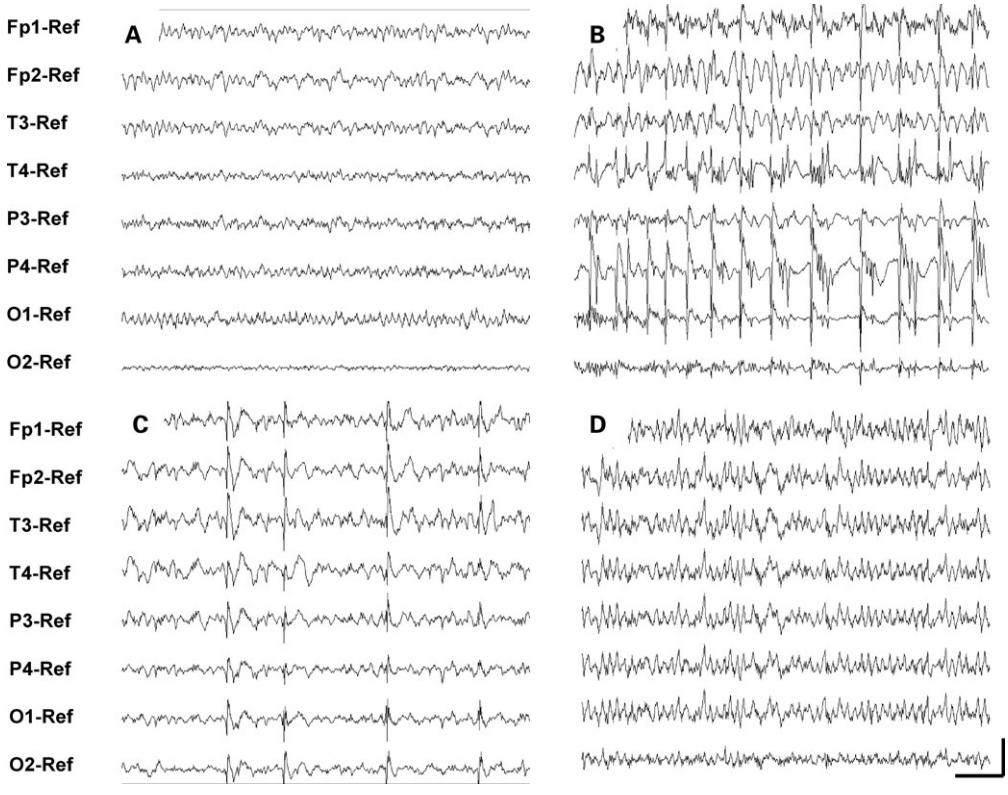

Figure 8. Prolonged electrocorticogram of *Rai1* mutants. (**A**) Background EEG of a freely moving wild-type mouse. (**B**) Example of a spontaneous seizure in a *Rai1* −/− mouse. (**C** and **D**) abnormal background and frequent interictal epileptiform discharges in *Rai1* +/− mice. Bars, 1 s and 500 mV. The individual recording intracranial electrode placement is as follows: Fp1, left frontopolar; Fp2, right frontopolar; T3, left temporal; T4, right temporal; O1, left occipital; O2, right occipital; Ref, reference.

6–7 Hz sharp waves that correlated with behavioral arrest. As the sharp waves gave way to generalized rhythmic 3 Hz spike and slow waves, an initial inactivity progressed into whole body clonic–tonic–clonic seizure lasting on average 30 seconds. Approximately 2% of *Rai1* +/− mice displayed overt seizures when they were over 4 months of age. However, even for the heterozygous mice without electrographic seizures recorded, VEEG showed an abnormal awake and sleep baseline electroencephalogram characterized by frequent epileptiform discharges (Fig. 8C and D).

DISCUSSION

We have genetically manipulated mice and generated several different models for SMS including mice with different

deletions and mice with targeted disruption in the single *Rai1* gene. Previous studies on body weight and craniofacial features indicated that *Rai1* +/− mice recapitulate the features of obesity and craniofacial abnormalities in mice with large or small deletions, indicating that dosage insufficiency of *RAI1* contributes to these features in SMS. Herein we characterized the behavioral features of mice with the small deletion, *Rai1* +/− mice and *Rai1* −/− mice, and compared these features with those of the large deletion mice and *Rai1* +/− mice reported previously. Our data indicate that mice with the small deletion showed the behavioral abnormalities as observed in the large deletion mice and the *Rai1* −/− mice display abnormalities in complex traits including motor functions and learning ability, whereas minimal behavioral abnormalities were observed in the *Rai1* +/− mice.

Del mice were hypoactive while the mice with reciprocal duplication were hyperactive (27). Hypoactivity was also observed in the small deletion mice in this study as indicated by significantly reduced travel time in the open field test. Thus, the ∼590 kb interval deleted in the small deletion mice contains the gene(s) or regulatory elements responsible for the abnormal locomotor activity in the Del mice. In the open-field test, the travel distance and travel time for the *Rai1* +/− mice were comparable with those in the wild-type littermates, suggesting that one copy of *Rai1* is enough for normal locomotive activity in the N2 generation. However, a previous study showed that the *Rai1* +/− mice generated by mating *Dp(11)17*/+ mice in a C57BL/6 background with *Rai1* +/− mice in a mixed C57BL/6 and 129SvEv genetic background (F2 generation) exhibited significantly decreased total travel distance and thus were hypoactive (14). This discrepancy suggests that variation in different genetic background substantially affects the penetrance and expressivity of behavioral phenotypes due to *Rai1* dosage effect. Of note, the *Rai1* +/− mice did display some neurobehavioral phenotypes even in the N2 background. The significantly increased exploratory vertical activity observed in N2 background herein is also observed in that study (14). In addition, ∼2% of *Rai1* +/− mice displayed overt seizures and an abnormal electroencephalograph (EEG) was observed in the *Rai1* +/− mice. Therefore, loss of one copy of *Rai1* compromises normal neural development and we propose that *Rai1* is at least partially responsible for the neurobehavioral phenotypes in the deletion mice.

We previously demonstrated that *Rai1* is dosage dependant in skeletal development; the skeletal abnormalities in *Rai1* −/− mice are much more severe than those observed in *Rai1* +/− mice (21). *Rai1* gene copy number variation as a cause of behavioral traits has been explored in a study to rescue the phenotypes in Dup mice through restoration of the normal disomic *Rai1* gene dosage in compound heterozygous mice carrying a *Dp(11)17* along with a null allele of *Rai1* (14). By examining the behavioral traits in the *Rai1* +/− and *Rai1* −/− mice, we provide direct evidence to show that the more reduced the copy number of *Rai1* in a mouse, the more severe the behavioral abnormalities including the learning disability, motor deficiency, and seizures. The deficits in both context associative and tone-dependent learning in conditioned fear tests were also observed in the small deletion mice and *Rai1* −/− mice but not in the *Rai1* +/− mice. One possible explanation for the more severe behavioral phenotypes in the deletion mice compared with the heterozygous knockout mice is that the expression of *Rai1* from the remaining normal allele in the small deletion mice is less than that in the *Rai1* +/− mice because of potential *trans*-regulatory elements in the deleted region. The reduced penetrance of craniofacial abnormalities in mice with the smaller deletion and *Rai1* +/− is also consistent with this interpretation (23). The contextual learning deficit is sensitive to lesions in the hippocampus where *Rai1* showed predominant expression in the neurons of both the cornu ammonis and dentate gyrus. Thus, the deficit in learning and memory may result from a hippocampus defect. Evaluation of long-term potentiation and long-term depression in hippocampal slices is necessary for delineation of the cellular mechanisms (28).

In the same N2 generation, the small deletion mice exhibited defective locomotor activity whereas the *Rai1* +/− mice were comparable with the wild-type. The *Rai1* allele in the knockout mice is a functional null allele and not likely a hypomorphic allele because sequences that encode the functional domains of nuclear localization and the PHD domain were included within the ∼4 kb deletion in the targeted allele (21). Furthermore, RT–PCR for *Rai1* using primers to the deleted and downstream regions revealed no transcripts (21); the absence of *Rai1* gene expression was also observed with whole genome expression arrays of *Rai1* −/− embryos (data not shown). Thus, we cannot exclude the involvement of modifiers located within the small deletion interval in contributing to behavioral traits. A previous study on the craniofacial abnormalities in SMS mouse models suggested that *trans* regulator(s) other than the *Rai1* in the SMS region can modify the penetrance of the craniofacial phenotype (23). Similarly, gene(s) or regulatory elements other than the *Rai1* coding sequences are involved in the behavioral phenotypes. The 11 genes other than the *Rai1* in the small deletion interval include *Rasd1* encoding a small G protein that has been shown to be a critical modulator in the circadian timekeeping system in mice (29). Behavioral studies on mice with these genes disrupted, with careful evaluation of the heterozygous mutants and double knockout of *Rai1* and individual genes in the small deletion, may help clarify the functions of these genes in behavior as assessed by objective testing.

It is interesting to note that impaired fear conditioning was present in the *Df(11)17 − 1* mice with ∼590 kb deletion and *Rai1* −/− mice but not in the Del mice with ∼2 Mb deletion although the ∼590 kb deletion is located within the 2 Mb region and the *Df(11)/17 − 1* mice and the Del mice were evaluated in the same background. During the training stage of the conditioned fear test, when a mild foot shock was applied the mice with the smaller deletion and the *Rai1* −/− mice manifested the same response as the wild-type mice such as running, jumping and vocalizing, suggesting that pain sensitivity of these mice is similar to the wild-type mice. Our previous studies showed that compound heterozygous Del/Dup mice have normal body weight and normal craniofacial features and are normal in the conditioned fear test (14), suggesting that the related phenotypes in the Del and Dup are due to gene dosage effects. Importantly, the restoration of the normal disomic *Rai1* gene dosage is sufficient to rescue the physical and behavioral phenotypes observed

in Del mice (14) indicating that *Rai1* is the dosage sensitive gene. Therefore, the impaired fear conditioning in the mice with smaller deletion is mainly caused by dosage insufficiency of *Rai1* plus the effect of genetic modifiers within the ~590 kb. This phenotype was inhibited in the Del mice by the deleted region outside of the 590 kb interval. Examination of the behavioral phenotypes in the compound heterozygous mice with the smaller deletion and Dup allele may help further elucidate this regional interaction.

In summary, our behavioral studies suggest that *Rai1* is a dosage sensitive gene required for normal behavioral function and *Rai1* copy number variation affects mouse behaviors with minimal behavioral abnormalities for one copy loss and severe motor and learning deficits for complete loss of *Rai1*. Gene(s) other than the *Rai1* or regulatory elements in the ~590 kb deleted in the small deletion mice modify the behavioral traits.

MATERIALS AND METHODS

Testing animals

Mice were housed under constant temperature, humidity and a light/dark cycle of 12 h (light 7:00 AM to 7:00 PM). All animal studies were conducted under protocols approved by the Baylor Institutional Animal Care and Use Committee and followed NIH guidelines. We separated the behavioral tests into two independent studies. Mice for both studies were around 3 months of age at the beginning of the testing. Experiments were conducted by an experimenter blinded to the genotypes of the mice. One study is to compare the behaviors of smaller deletion mice and the *Rai1* +/− mice with that of the large deletion mice. Mice were tested in the mixed (75% C57BL/6 and 25% 129SvEv) genetic background at the N2 generation. Twenty-one small deletion males and 20 wild-type male littermates were evaluated in the open-field, light–dark, prepulse inhibition of the startle response and conditioned fear test. The same battery of tests was performed on 19 *Rai1* +/− males and 19 wild-type male littermates.

Another study sought to explore the behavioral defects in the *Rai1* −/− mutants. Mice were maintained on a mixed (50% C57BL/6 and 50% 129SvEv) background. Mice with different genotypes were housed with their littermates but with males and females separately. Data used for statistical analysis are from tests of 8 (5 females and 3 males) *Rai1* −/− mutants, 15 (5 females and 10 males) *Rai1* +/− mutants and 12 (6 females and 6 males) wild-type mice.

Motor function test

Motor skills were evaluated by rotating rod test, vertical pole test, suspended wire test and dowel test. For the rotating rod test, mice were placed on a rotating rod (model 7650 Rota-rod, Ugo Basile) that accelerated from 3 to 30 rpm. The mice were given one training trial 2 h before the test. For four consecutive days, four trials were performed per day with 45–60 min interval between trials. The maximum duration of each trial was 10 min. The time that the mice fell off the rod was recorded. For the vertical pole test, mice were placed on one end of a pole (1.9 cm diameter, 43 cm length). The pole was shifted to a vertical position. A score was given based on the position of the pole and the time that the mice remained on the pole (30). The wire test was implemented by suspending mice with their forepaws on a 2 mm wire, and the amount of time they stayed on the wire was recorded in a 60 s interval. For the dowel test, mice were placed in the center of a horizontal wooden dowel (0.9 cm diameter) suspended between two platforms. The time that the mice remained on the dowel was recorded in a 60 s interval.

Conditioned fear test

The fear conditioning was conducted in a test chamber (26 × 22 × 18 cm) with a grid floor used to deliver an electric foot shock. The chamber was placed inside a sound-attenuating chest (56 × 38 × 36 cm) with a peep hole on one side of the door to allow the observation of mouse behaviors. The chamber was cleaned with 100% ethanol before each mouse was placed inside. Freezing was assessed as 1 (freezing posture) or 0 (no freezing posture) and the scores were averaged over 10 s intervals and converted to a percentage score. One mouse was placed in the chamber for 2 min to get familiar with the chamber. An 80 dB white noise was present for 30 s, which serves as the conditioned stimulus (CS). A mild foot shock (2 s, 0.5 mA) was followed, which serves as the unconditioned stimulus (US). After 2 min, another CS–US pair was provided. The mouse was placed back to its home cage after 30 s. Twenty-four hours later, the mouse was placed in the test chamber and freezing behavior was recorded every 10 s for 5 min (context test). For auditory CS test, mice were placed in the same chamber with environment and contextual cues alternated by changing light color, space size, smell and floor. Freezing was recorded for 3 min without CS (pre-CS phase) and for another 3 min with the continuous auditory CS (CS phase).

Open-field test, light–dark exploration and prepulse inhibition

Mice were placed in the center of an open-field space (40 × 40 × 30 cm) and allowed to explore freely for 30 min. Activities were quantitated by a computer-operated Digiscan optical animal activity system (RXYZCM, Accuscan Electronics). Data were collected over 2 min intervals during a 30 min test session. Light–dark exploration test and startle and prepulse inhibition of the startle were performed as described (25).

EEG recordings

Mice were anesthetized with avertin, and teflon-coated silver wire electrodes (0.005 in diameter) were implanted bilaterally into the subdural space over the frontal, temporal parietal and occipital cortexes at least 24 h before recording. The electrodes were soldered to a microminiature connector. EEG activity was recorded on mice moving freely in the test cage during random 2–24 h samples for 7–10 days using a digital VEEG (Stellate Harmonie).

Histology, immunohistochemistry and X-gal staining

Adult mice were anesthetized with avertin and the brains were dissected and fixed with 10% formalin for at least 24 h. The tissues were then washed, embedded in paraffin, sectioned and stained with hematoxylin and eosin. For immunohistochemistry, brains were cut sagittally in half and embedded in frozen tissue matrix (optimal cutting temperature compound OCT, tissue-Tek). Sections of 15 μm were sliced using a cryostat (Microm HM500) and stored in −80°C. Sections were fixed in 1:1 acetone: methanol for 10 min. Rabbit polyclonal anti-beta-galactosidase antibody (Cortex Biochem, San Leandro, CA) was diluted at 1:200 in 10% goat serum-PBS. Mouse anti-Neuronal Nuclei (NeuN) monoclonal antibody (Chemicon, Temecula, CA) was diluted at 1:100. The secondary antibodies are Goat anti-rabbit Alexa Fluor 594, and Rabbit anti-mouse Alexa Fluor 488 (Molecular probes, Carlsbad, CA) diluted at 1:200. Sections were mounted in Slow-Fade Antifade (Molecular Probes, Carlsbad, CA). For X-gal staining, frozen sections were air-dried for 5 min and stained as described before (21) with the exception that the staining was performed in 37°C overnight in darkness. After staining, the sections were washed and counter-stained with fast red.

Statistical analysis

Except for the pole test, behavior data were analyzed using ANOVA with appropriate follow-up comparisons of the main effect. The pole test data were analyzed using the non-parametric Mann–Whitney *U* test.

Web resources

Accession numbers and URLs for data presented herein are as follows:

On line Mendelian Inheritance in Man (OMIM), http://www.ncbi.nlm.nih.gov/Omim/.

Allen Brain Atlas (ABA), http://www.brain-map.org/welcome.do/.

SUPPLEMENTARY MATERIAL

Supplementary Material is available at HMG Online.

ACKNOWLEDGEMENTS

We thank Drs L. Luo and K. Walz for critical reviews. This work was supported in part by grants from the National Institute for Dental and Craniofacial Research (R01 DEO15210), the Mouse Physiology Core and the Neurobehavioral Core of the Baylor Mental Retardation and Developmental Disabilities Research Center (P30 HD 24064) and a grant from the March of Dimes (J.R.L. and W.B.).

Conflict of Interest statement. None declared.

REFERENCES

1. Greenberg, F., Lewis, R.A., Potocki, L., Glaze, D., Parke, J., Killian, J., Murphy, M.A., Williamson, D., Brown, F., Dutton, R. *et al.* (1996) Multi-disciplinary clinical study of Smith–Magenis syndrome (deletion 17p11.2). *Am. J. Med. Genet.*, **62**, 247–254.
2. Smith, A.C.M., McGavran, L., Robinson, J., Waldstein, G., Macfarlane, J., Zonona, J., Reiss, J., Lahr, M., Allen, L. and Magenis, E. (1986) Interstitial deletion of (17)(p11.2p11.2) in nine patients. *Am. J. Med. Genet.*, **24**, 393–414.
3. Stratton, R.F., Dobyns, W.B., Greenberg, F., DeSana, J.B., Moore, C., Fidone, G., Runge, G.H., Feldman, P., Sekhon, G.S., Pauli, R.M. *et al.* (1986) Interstitial deletion of (17)(p11.2p11.2): report of six additional patients with a new chromosome deletion syndrome. *Am. J. Med. Genet.*, **24**, 421–432.
4. Bi, W. and Lupski, J.R. (2007) *RAI1*,the Smith–Magenis and dup(17)(p11.2p11.2)syndromes. In Epstein, C.J., Erickson, R.P. and Wynshaw-Boris, A. (eds), *Inborn Errors of Development*, Oxford University Press, New York, in press.
5. Greenberg, F., Guzzetta, V., Montes de Oca-Luna, R., Magenis, R.E., Smith, A.C.M., Richter, S.F., Kondo, I., Dobyns, W.B., Patel, P.I. and Lupski, J.R. (1991) Molecular analysis of the Smith–Magenis syndrome: a possible contiguous-gene syndrome associated with del(17)(p11.2). *Am. J. Hum. Genet.*, **49**, 1207–1218.
6. Madduri, N., Peters, S.U., Voigt, R.G., Llorente, A.M., Lupski, J.R. and Potocki, L. (2006) Cognitive and adaptive behavior profiles in Smith–Magenis syndrome. *J. Dev. Behav. Pediatr.*, **27**, 188–192.
7. Chen, K.-S., Manian, P., Koeuth, T., Potocki, L., Zhao, Q., Chinault, A.C., Lee, C.C. and Lupski, J.R. (1997) Homologous recombination of a flanking repeat gene cluster is a mechanism for a common contiguous gene deletion syndrome. *Nat. Genet.*, **17**, 154–163.
8. Bi, W., Yan, J., Stankiewicz, P., Park, S.-S., Walz, K., Boerkoel, C.F., Potocki, L., Shaffer, L.G., Devriendt, K., Nowaczyk, M.J.M. *et al.* (2002) Genes in a refined Smith–Magenis syndrome critical deletion interval on chromosome 17p11.2 and the syntenic region of the mouse. *Genome Res.*, **12**, 713–728.
9. Zody, M.C., Garber, M., Adams, D.J., Sharpe, T., Harrow, J., Lupski, J.R., Nicholson, C., Searle, S.M., Wilming, L., Young, S.K. *et al.* (2006) DNA sequence of human chromosome 17 and analysis of rearrangement in the human lineage. *Nature*, **440**, 1045–1049.
10. Bi, W., Saifi, G.M., Shaw, C.J., Walz, K., Fonseca, P., Wilson, M., Potocki, L. and Lupski, J.R. (2004) Mutations of RAI1, a PHD-containing protein, in nondeletion patients with Smith–Magenis syndrome. *Hum. Genet.*, **115**, 515–524.
11. Slager, R.E., Newton, T.L., Vlangos, C.N., Finucane, B. and Elsea, S.H. (2003) Mutations in *RAI1* associated with Smith–Magenis syndrome. *Nat. Genet.*, **33**, 466–468.
12. Girirajan, S., Elsas, L.J., II, Devriendt, K. and Elsea, S.H. (2005) RAI1 variations in Smith–Magenis syndrome patients without 17p11.2 deletions. *J. Med. Genet.*, **42**, 820–828.
13. Bi, W., Saifi, G.M., Girirajan, S., Shi, X., Szomju, B., Firth, H., Magenis, R.E., Potocki, L., Elsea, S.H. and Lupski, J.R. (2006) *RAI1* point mutations, CAG repeat variation, and SNP analysis in non-deletion Smith–Magenis syndrome. *Am. J. Med. Genet. A*, **140**, 2454–2463.
14. Walz, K., Paylor, R., Yan, J., Bi, W. and Lupski, J.R. (2006) *Rai1* duplication causes physical and behavioral phenotypes in a mouse model of dup(17)(p11.2p11.2). *J. Clin. Invest.*, **116**, 3035–3041.
15. Bi, W., Park, S.-S., Shaw, C.J., Withers, M.A., Patel, P.I. and Lupski, J.R. (2003) Reciprocal crossovers and a positional preference for strand exchange in recombination events resulting in deletion or duplication of chromosome 17p11.2. *Am. J. Hum. Genet.*, **73**, 1302–1315.
16. Potocki, L., Chen, K.-S., Park, S.-S., Osterholm, D.E., Withers, M.A., Kimonis, V., Summers, A.M., Meschino, W.S., Anyane-Yeboa, K., Kashork, C.D. *et al.* (2000) Molecular mechanism for duplication 17p11.2—the homologous recombination reciprocal of the Smith–Magenis microdeletion. *Nat. Genet.*, **24**, 84–87.
17. Potocki, L., Bi, W., Treadwell-Deering, D., Carvalho, C.M., Eifert, A., Friedman, E.M., Glaze, D., Krull, K., Lee, J.A., Lewis, R.A. *et al.* (2007) Characterization of Potocki–Lupski Syndrome (dup(17)(p11.2p11.2)) and delineation of a dosage-sensitive critical interval that can convey an autism phenotype. *Am. J. Hum. Genet.*, **80**, 633–649.
18. Hayes, S., Turecki, G., Brisebois, K., Lopes-Cendes, I., Gaspar, C., Riess, O., Ranum, L.P.W., Pulst, S.-M. and Rouleau, G.A. (2000) CAG repeat length in *RAI1* is associated with age at onset variability in spinocerebellar ataxia type 2 (SCA2). *Hum. Mol. Genet.*, **9**, 1753–1758.

19. Joober, R., Benkelfat, C., Toulouse, A., Lafrenière, R.G.A., Lal, S., Ajroud, S., Turecki, G., Bloom, D., Labelle, A., Lalonde, P. *et al.* (1999) Analysis of 14 CAG repeat-containing genes in schizophrenia. *Am. J. Med. Genet.*, **88**, 694–699.
20. Imai, Y., Suzuki, Y., Matsui, T., Tohyama, M., Wanaka, A. and Takagi, T. (1995) Cloning of a retinoic acid-induced gene, GT1, in the embryonal carcinoma cell line P19: neuron-specific expression in the mouse brain. *Mol. Brain. Res.*, **31**, 1–9.
21. Bi, W., Ohyama, T., Nakamura, H., Yan, J., Visvanathan, J., Justice, M.J. and Lupski, J.R. (2005) Inactivation of *Rai1* in mice recapitulates phenotypes observed in chromosome engineered mouse models for Smith–Magenis syndrome. *Hum. Mol. Genet.*, **14**, 983–995.
22. Walz, K., Caratini-Rivera, S., Bi, W., Fonseca, P., Mansouri, D.L., Lynch, J., Vogel, H., Noebels, J.L., Bradley, A. and Lupski, J.R. (2003) Modeling del(17)(p11.2p11.2) and dup(17)(p11.2p11.2) contiguous gene syndromes by chromosome engineering in mice: phenotypic consequences of gene dosage imbalance. *Mol. Cell. Biol.*, **23**, 3646–3655.
23. Yan, J., Bi, W. and Lupski, J.R. (2007) Penetrance of craniofacial anomalies in mouse models of Smith–Magenis syndrome is modified by genomic sequence surrounding *Rai1*—not all null alleles are alike. *Am. J. Hum. Genet.*, **80**, 518–525.
24. Yan, J., Keener, V.W., Bi, W., Walz, K., Bradley, A., Justice, M.J. and Lupski, J.R. (2004) Reduced penetrance of craniofacial anomalies as a function of deletion size and genetic background in a chromosome engineered partial mouse model for Smith–Magenis syndrome. *Hum. Mol. Genet.*, **13**, 2613–2624.
25. Walz, K., Spencer, C., Kaasik, K., Lee, C.C., Lupski, J.R. and Paylor, R. (2004a) Behavioral characterization of mouse models for Smith-Magenis syndrome and dup(17)(p11.2p11.2). *Hum. Mol. Genet.*, **13**, 367–378.
26. Paylor, R., Nguyen, M., Crawley, J.N., Patrick, J., Beaudet, A. and Orr-Urtreger, A. (1998) Alpha7 nicotinic receptor subunits are not necessary for hippocampal-dependent learning or sensorimotor gating: a behavioral characterization of Acra7-deficient mice. *Learn. Mem.*, **5**, 302–316.
27. Walz, K., Fonseca, P. and Lupski, J.R. (2004b) Murine models for human contiguous gene syndromes and other genomic disorders. *Genet. Mol. Biol.*, **27**, 305–320.
28. Stevens, C.F. (1998) A million dollar question: does LTP = memory? *Neuron*, **20**, 1–2.
29. Cheng, H.Y., Obrietan, K., Cain, S.W., Lee, B.Y., Agostino, P.V., Joza, N.A., Harrington, M.E., Ralph, M.R. and Penninger, J.M. (2004) Dexras1 potentiates photic and suppresses nonphotic responses of the circadian clock. *Neuron*, **43**, 715–728.
30. Shahbazian, M., Young, J., Yuva-Paylor, L., Spencer, C., Antalffy, B., Noebels, J., Armstrong, D., Paylor, R. and Zoghbi, H. (2002) Mice with truncated MeCP2 recapitulate many Rett syndrome features and display hyperacetylation of histone H3. *Neuron*, **35**, 243–254.